



Steady State Performance of Spark Ignition Engine with Exhaust Energy Recovery

Emiliano Pipitone and Salvatore Caltabellotta University of Palermo

Citation: Pipitone, E. and Caltabellotta, S., "Steady State Performance of Spark Ignition Engine with Exhaust Energy Recovery," SAE Technical Paper 2020-24-0012, 2020, doi:10.4271/2020-24-0012.

Abstract

As is known, internal combustion engines based on Otto or Diesel cycles cannot complete the expansion process of the gas inside the cylinder, thus losing a relevant energy content, in the order of 30% of total. The residual energy of the unexpanded gas has been partially exploited through the use of an exhaust gas turbine for turbocharging the internal combustion engine; further attempts have been made with several compound solutions, with an electric generator connected to the turbocharger allowing to convert into electrical energy the quota power produced by the turbine which is not used by the compressor, or with a second turbine downstream the first to increase the exhaust gas energy recovery. Turbo-compound solutions were also employed in large marine Diesel engines, where the second turbine downstream the first was used to deliver more power to the main propeller shaft. In all these cases the overall efficiency increments remained within 5%. If completely

recovered by the use of a properly designed expander-generator unit, the energy content of the unexpanded in-cylinder gas could substantially increase the overall efficiency of the thermal unit. In the present paper the authors evaluate, by means of simple yet effective calculations, the efficiency attainable by a thermal unit composed of a spark ignition engine endowed of an exhaust gas energy recovery expander connected to a proper generator. The proposed thermal unit, which is particularly suitable for hybrid propulsion solutions, has been evaluated both in the naturally aspirated and in the supercharged version. The efficiency of each thermal unit is also compared to reference baseline engine, thus highlighting the real benefit introduced by the adoption of the proposed thermal unit. As result, it was found that the complete and efficient recovery of the unexpanded gas energy has the potential to increase the overall efficiency of the propulsion system by 10-15%, depending on the characteristics of the thermal engine and of the exhaust energy expander-generator unit.

Introduction

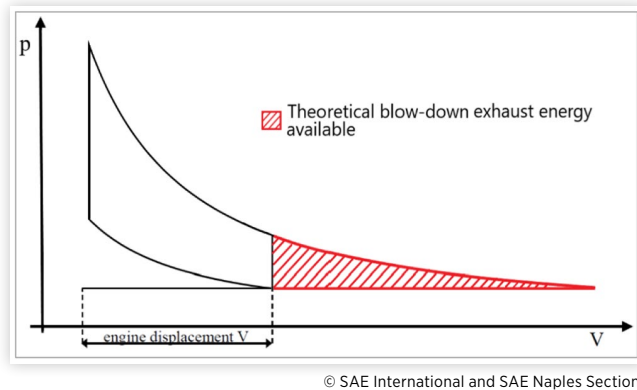
Recent concerns regarding environmental issues and increasingly evident climate changes highlight the need to adopt appropriate measures for the consumption reduction of oil derived fuels. Besides the increased concentration of CO₂ in the atmosphere, the combustion of fossil fuels, typically in the energy conversion processes (electrical, thermal) and in the transport sector, is also among the major causes of environmental pollution. EU policy addresses far-reaching topics such as climate change produced by transport sector. As stated in the "White Paper" the European Union needs to drastically reduce greenhouse gas emissions worldwide, with the aim of keeping global warming below 2°C [1]. To achieve its objectives, EU affirms that, by 2050, transport emissions must be reduced by 60% compared to 1990 levels [2]. In an attempt to meet these expectations, great attention is paid to the transport sector with the aim of being able to make vehicles more adequate to comply with current and future environmental regulations, above all increasing exploitation of gaseous fuels [3] and bio-fuels. The increasingly restrictive anti-pollution regulations all over the world and the progressive growth of hydrocarbon fuels cost are

pushing towards market solutions combining the respect for the environment with the vehicle fuel economy. Hybrid electric vehicles (HEV) revealed quite competitive, allowing significantly fuel consumption reduction compared to traditional internal combustion engine vehicles (ICEV), especially in urban areas. Their development is relatively recent and there are still room for improvement. A possible working area is represented by the internal combustion engine, which, if based on Otto or Diesel cycles, cannot complete the expansion process of the gas inside the cylinder, thus losing a relevant energy content, in the order of 30% of total, as shown in [Figure 1](#), where the red dashed area represents the energy content of the unexpanded gas in an ideal Otto cycle.

To date, several systems for the recovery of this energy content have been already studied and proposed. The most common in the automotive sector is represented by the use of a turbine for turbocharging the internal combustion engine: in this case, as known, the turbine produce only the power required by the turbocompressor, thus strongly reducing the exhaust energy recovery.

Several systems have been proposed in the scientific literature for the efficient exploitation of the energy resource

FIGURE 1 Energy related to the incomplete gas expansion in an Otto cycle.

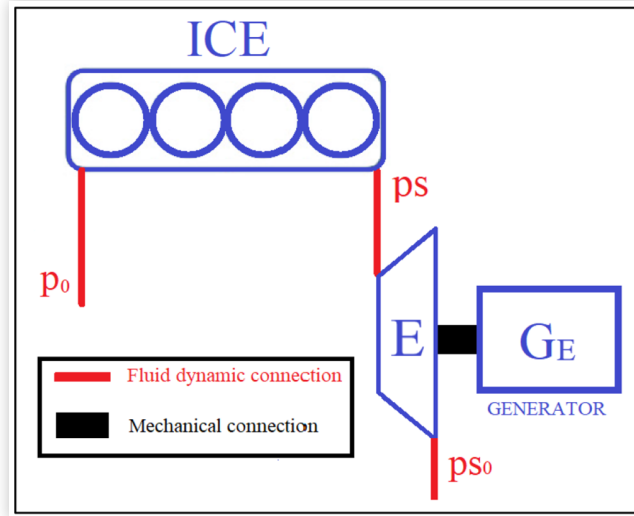


of the engine exhaust gas [4, 5, 6]. Some systems focused on engine turbocharger with the aim to recover the amount of power produced by the turbine but not required by the turbo-compressor [7, 8, 9, 10]; in these systems, commonly referred to as electrical turbo-compound, an electrical motor/generator has been installed on the turbocharger shaft thus allowing a partial recovery of the unused exhaust gas power: as a result, overall efficiency increase not higher than 6% were obtained. Other systems instead considered the application of an auxiliary turbo-generator (i.e. a turbine connected to an electrical generator) downstream the first turbine (of the engine turbocharger) [11, 12], reaching however fuel economy improvement within 4%. It is worth noting that "turbo-compound" with a second turbine downstream the first have been first employed in marine propulsion systems to increase the energy efficiency and add more power on the main propeller shaft. A different approach was followed by [13, 14], since the auxiliary turbo-generator was installed in parallel to first turbine (engine turbocharger): in both cases, fixed geometry and variable geometry turbine were employed, obtaining efficiency improvement up to 9%.

In this paper the authors propose a different approach, with the purpose to perform a complete and efficient recovery of the unexpanded gas energy. As shown in Figure 2, the thermal unit considered by the authors is composed by a spark ignition engine whose exhaust gas are directly conveyed in a proper exhaust gas expander (E) connected to an electrical generator (G_E): the difference with the systems already studied is that in the proposed thermal unit the whole exhaust gas from the internal combustion engine completes the expansion (from the engine exhaust pressure p_s to the exhaust pipe pressure p_{so}) inside the expander whose output power is transformed into electric power by the generator.

The system conceived is particularly suitable for hybrid propulsion systems for different reason; the application to a traditional internal combustion engine vehicle (ICEV), in effect, would require a mechanical connection between the expander and the engine output shaft, which would result nor efficient neither practical, given the difference between the speed of rotation, which, in a traditional ICEV, would not remain constant; in a hybrid architecture, instead, the two elements may operate separately, and the respective power can be easily summed up in the energy storage system; moreover,

FIGURE 2 Schematic representation of the proposed thermal unit



in a hybrid propulsion system, the operative conditions of the thermal engine does not change as in a traditional vehicle, and this would let the expander to work under quasi-steady conditions, with great benefit in terms of expansion efficiency. To this purpose, the research carried out in [15] is quite relevant since focuses on a stand-alone exhaust gas turbo-generator which could be profitably employed in the thermal unit proposed. In a hybrid propulsion system [16], the additional electric power produced by the expander-generator group could hence contribute to the total power delivered by the engine, thus increasing the fuel economy of the vehicle.

The research carried out in this paper aims to evaluate the advantages connected by the implementation of the proposed thermal unit in a hybrid propulsion system. To this purpose, the steady state performance of the thermal unit proposed were compared to the performance of a baseline engine; the comparison was carried out considering both naturally aspirated and supercharged internal combustion engines and is based on an equal power basis, i.e. each engine and thermal unit was sized so as to deliver the same continuous maximum power of 73.5 kW (i.e. 100 HP).

It must be also pointed out that the system described in this paper has never been studied in the scientific literature: it was mentioned in [17] among the several different systems that could be simulated, but no energetic or performance evaluations were performed, nor a comparison was carried out with respect to traditional internal combustion engine. Several other differences can be observed with respect to [17], which will be pointed out further on in the paper.

Baseline Naturally Aspirated Engine

As first step, the steady state performances of the baseline engine were delineated; consequently, the steady state performance attainable by the proposed thermal units were

evaluated and compared to the baseline engine. Considering the application of the proposed system to future propulsion system, the purpose of the author was to perform efficiency comparison based on modern engines, equipped with the technology level which characterizes the European Type C - Medium passenger cars: according to this approach, a gasoline direct injection spark ignition engine with VVT system was considered as the reference technology level. Unfortunately this kind of engine was not available to the authors for proper experimental measurements, nor it was possible to trace any literature reference producing the required performance and fuel consumption map: on account of this data unavailability, the authors decided to build-up the baseline naturally aspirated engine performance combining some reference values of the brake thermal efficiency or mechanical efficiency, with performance curve experimentally measured on an available spark ignition engine and normalized to be representative of a generic engine: the normalized curve were hence adjusted according to the maximum values that were assumed coherently with the technology level of the engine considered.

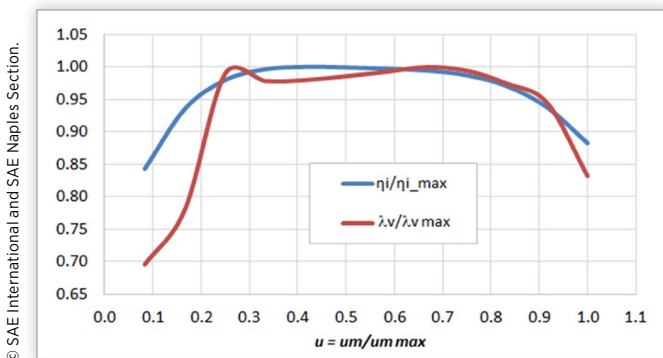
The first engine parameter taken into consideration is the indicated thermal efficiency η_i . Its typical trend was obtained by means of experimental measurements carried out in full load conditions on a spark ignition engine at different engine speed, or, which is equal, at different mean piston speed u_m : a double normalization procedure allowed hence to obtain the normalized indicated thermal efficiency ($\eta_i/\eta_{i,max}$) as a function of the normalized mean piston speed ($u_m/u_{m,max}$), as reported in [Figure 3](#). The same figure also shows the curve of the normalized engine volumetric efficiency ($\lambda_v/\lambda_{v,max}$) as function of the normalized mean piston speed. Assuming the normalized mean piston speed variable u :

$$u = \frac{u_m}{u_{m,max}} \quad (0 \leq u \leq 1) \quad (1)$$

the normalized indicated thermal efficiency was expressed by means of a proper polynomial:

$$\frac{\eta_i}{\eta_{i,max}} = 1.97 \cdot u^5 - 8.31 \cdot u^4 + 12.1 \cdot u^3 - 8.20 \cdot u^2 + 2.64 \cdot u + 0.67 \quad (2)$$

FIGURE 3 Normalized indicated thermal efficiency and volumetric efficiency as function of the normalized mean piston speed (full load condition)



while the normalized volumetric efficiency was expressed by:

$$\frac{\lambda_v}{\lambda_{v,max}} = 1228.15 \cdot u^8 - 5722.58 \cdot u^7 + 11160.9 \cdot u^6 - 11806.6 \cdot u^5 + 7327.04 \cdot u^4 - 2685.92 \cdot u^3 + 552.31 \cdot u^2 - 55.01 \cdot u + 2.6713 \quad (3)$$

The curve of the brake thermal efficiency η_b of the engine was instead obtained at the mid piston speed condition (i.e. $u = 0.5$) for different engine loads. Assumed ψ as the normalized load variable:

$$\psi = \frac{BMEP}{BMEP_{max}} \quad (0 \leq \psi \leq 1) \quad (4)$$

the normalized brake thermal efficiency ($\eta_b/\eta_{b,max}$) at the mid piston speed condition $u = 0.5$ is represented by the polynomial:

$$\left(\frac{\eta_b}{\eta_{b,max}} \right)_{u=0.5} = -3.51 \cdot \psi^5 + 4.85 \cdot \psi^4 + 2.06 \cdot \psi^3 - 6.75 \cdot \psi^2 + 4.20 \cdot \psi + 0.0650 \quad (5)$$

With the aim to pass from normalized curve to effective curve, a reference value was assumed for each fundamental parameter coherently with the technological level considered for the baseline naturally aspirated engine (endowed of GDI and VVT systems).

Employing the reference values listed in [Table 1](#), the volumetric efficiency of the engine for each mean piston speed can be evaluated by [equations \(3\)](#), while the brake thermal efficiency at $u = 0.5$ and for each normalized load is obtained by [equation \(5\)](#); the latter obviously allows to determine the brake thermal efficiency at full load (i.e. 0.318 at $\psi = 1$ and $u = 0.5$), and hence to establish a reference value

FIGURE 4 Normalized brake thermal efficiency as function of the normalized load, at mid piston speed condition

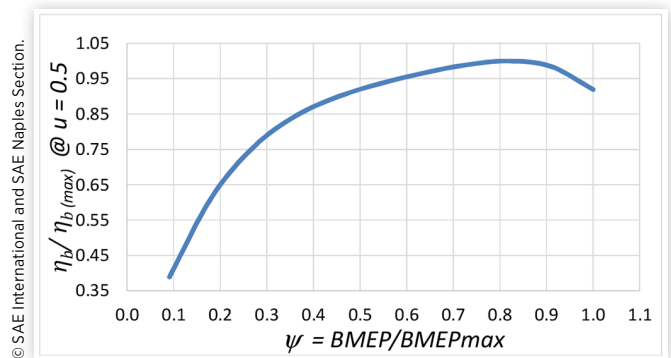
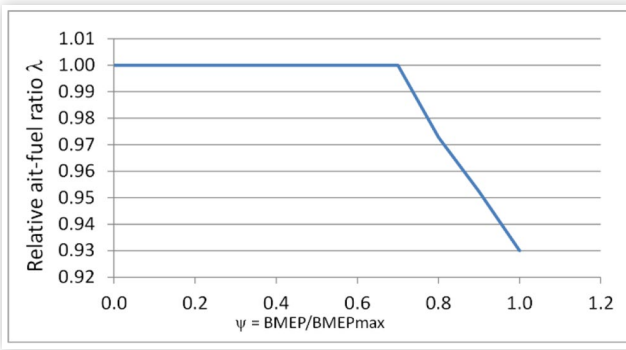


TABLE 1 Reference values adopted for the performance parameters of the baseline naturally aspirated engine

$u_{m,max}$ [m/s]	17
$\eta_{b,max}$ @ $u = 0.5$	0.346
η_m @ $\psi = 1$ $u = 0.5$	0.860
$\lambda_{v,max}$	1.00

FIGURE 5 Relative air-fuel ratio as function of engine load

also for the indicated efficiency at full load ($\psi = 1$) and mid speed ($u = 0.5$):

$$\eta_i(\psi = 1, u = 0.5) = \frac{0.318}{0.860} = 0.370 \quad (6)$$

which, in turn, allows to obtain the real indicated efficiency curve from the normalized curve of equation (2).

The data available at this point allow determining the IMEP at full load and for each mean piston speed:

$$IMEP = \frac{\delta_0 \cdot \lambda_V \cdot LHV}{\lambda \cdot \alpha_{st}} \cdot \eta_i \quad (7)$$

being δ_0 the air density in the intake manifold (1.17 kg/m^3 for full load operation at standard conditions), LHV the lower heating value of the fuel (43 MJ/kg for gasoline), α_{st} the fuel stoichiometric air-fuel ratio (14.7 for gasoline) and λ the relative air-fuel ratio, whose trend as function of engine load is shown in Figure 5.

As regards the overall mechanical efficiency η_m :

$$\eta_m = \frac{BMEP}{IMEP} = \frac{IMEP - FMEP}{IMEP} = 1 - \frac{FMEP}{IMEP} \quad (8)$$

the authors followed a Chen-Flynn approach. The friction mean effective pressure (FMEP) was considered function of the IMEP (assumed here as the pressure-load related variable in place of the maximum in-cylinder pressure) and of the mean piston speed u_m :

$$FMEP = A + B \cdot IMEP + C \cdot u_m + D \cdot u_m^2 \quad (9)$$

being A , B , C and D the constants of the model. From equation (4) and (8), it derives that:

$$\eta_m = 1 - \frac{A + B \cdot IMEP + C \cdot u_m + D \cdot u_m^2}{IMEP} \quad (10)$$

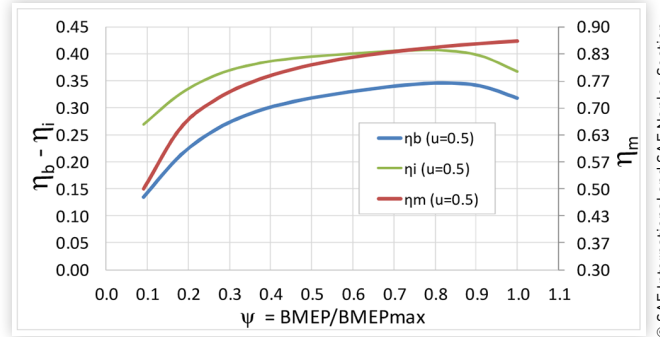
Four different values of the overall mechanical efficiency, corresponding to the four different conditions of load and speed reported in Table 2, were assumed on the basis of the data reported in [18]: this allowed determining the values of the constants A , B , C and D of the mechanical friction model employed.

The set of curves determined hence allowed to completely describe the engine efficiency and performance at each speed or load. As example, Figure 6 shows, for the mid speed

TABLE 2 Reference values of the mechanical efficiency

IMEP [bar]	u_m [m/s]	η_m [-]	IMEP/IMEPmax[-]	u [-]
13.1	8.50	0.865	1.00	0.50
9.81	17.0	0.770	0.75	1.00
7.89	4.25	0.861	0.60	0.25
2.07	8.50	0.500	0.16	0.50

© SAE International and SAE Naples Section.

FIGURE 6 Brake, indicated and mechanical efficiency as function of normalized load

© SAE International and SAE Naples Section.

condition $u=0.5$, the progress of the three efficiencies as function of normalized load.

Once the progress of volumetric efficiency, indicated efficiency and mechanical efficiency are known for the full load condition ($\psi=1$), the brake mean effective pressure of the engine may be calculated for each mean piston speed:

$$BMEP = \frac{\delta_0 \cdot \lambda_V \cdot LHV}{\lambda \cdot \alpha_{st}} \cdot \eta_i \cdot \eta_m \quad (11)$$

The result of the calculation provides the full load BMEP curve, whose maximum value of 11.75 bar allows to size the engine with the aim to obtain the output power of 73.5 kW . The displacement required V_A results to be 1566 cc . Considering that for passenger car engine the single cylinder displacement should remain within 0.5 L , and supposing a stroke to bore ratio of 1 , the main characteristics of engine result to be determined, as resumed in Table 3:

The volumetric compression ratio of 11 was selected according to the technology level of the engine considered (Spark Ignition, $4V/\text{cylinder}$, GDI, VVT). The engine fuel consumption, both brake and indicated, can be obtained as:

$$BSFC_{[g/kWh]} = \frac{3600}{LHV_{[MJ/kg]} \cdot \eta_b} = \frac{\delta_0_{[kg/m^3]} \cdot \lambda_V \cdot 36000}{BMEP_{[bar]} \cdot \lambda \cdot \alpha_{st}} \quad (12)$$

$$ISFC_{[g/kWh]} = \frac{3600}{LHV_{[MJ/kg]} \cdot \eta_i} = \frac{\delta_0_{[kg/m^3]} \cdot \lambda_V \cdot 36000}{IMEP_{[bar]} \cdot \lambda \cdot \alpha_{st}} \quad (13)$$

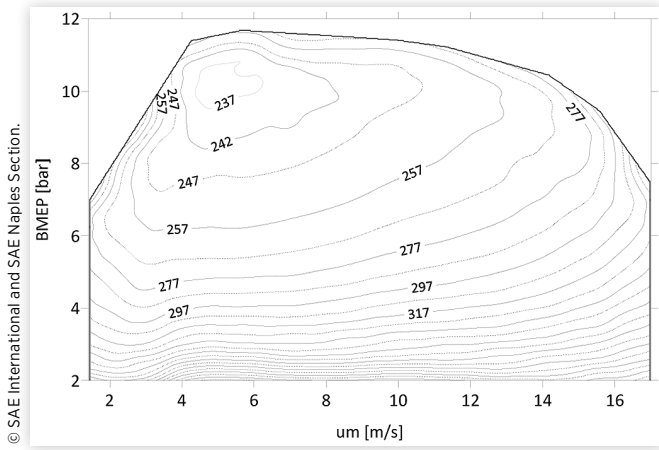
The BSFC allows tracing the fuel consumption map of the engine, reported in Figure 7.

It is worth noting that up to this point the net IMEP was always considered (equations (7) (8) and (13)), even if some calculations may require the use of the gross indicated mean effective pressure $IMEP_g$ which leaves a part the gas exchange phases and takes into account the gross indicated work, i. e.

TABLE 3 Main characteristics of the baseline engine

Engine	4-stroke, naturally aspirated, spark ignition
Displacement	1566 cc
Number of Cylinders	4
Bore	79.3 mm
Stroke	79.3 mm
Compression Ratio	11
Injection system	Gasoline direct injection
Valvetrain	4 valves/cylinder, VVT
Max BMEP	11.75 bar at 2100 rpm
Max Power	73.5 kW at 5400 rpm
Min BSFC	236.9 g/kWh

© SAE International and SAE Naples Section.

FIGURE 7 Brake specific fuel of the baseline naturally aspirated engine


© SAE International and SAE Naples Section.

the work exchanged between piston and gas during the compression and expansion strokes only:

$$IMEP_g = IMEP - PMEP \quad (14)$$

The pumping mean effective pressure PMEP is approximately evaluated as:

$$PMEP = MAP - p_{s0} \quad (15)$$

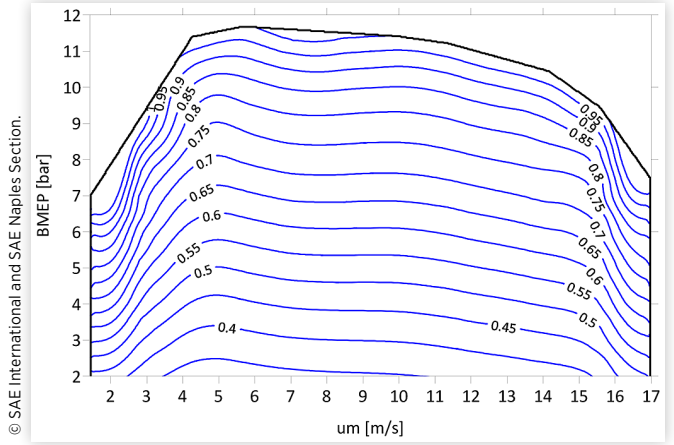
where the exhaust pressure for the baseline engine p_{s0} was considered constant and $= 1.06 p_0$, while the manifold absolute pressure MAP is related to the BMEP through the manifold air density δ_0 , which depends on the temperature T_0 in the manifold:

$$\delta_0 = \frac{MAP}{R' \cdot T_0} \quad (16)$$

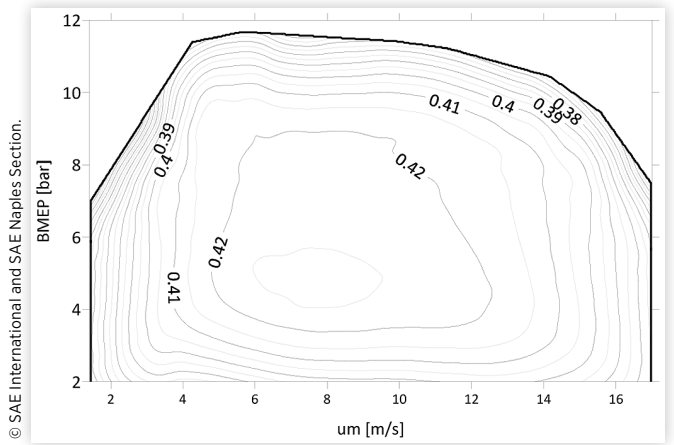
For the full load condition, δ_0 is the air density at the ambient condition (1.169 kg/m^3 at 1 bar and 298 K), while in part load operation, the required MAP can be evaluated for each desired BMEP:

$$MAP = \frac{BMEP \cdot R' \cdot T_0 \cdot \lambda \cdot \alpha_{st}}{\lambda_v \cdot LHV \cdot \eta_i \cdot \eta_m} \quad (17)$$

Figure 8 reports the MAP values necessary for each load ($BMEP$) and speed (u_m) of the naturally aspirated baseline engine.

FIGURE 8 Manifold absolute pressure as function of BMEP and u_m (baseline naturally aspirated engine)


© SAE International and SAE Naples Section.

FIGURE 9 Gross indicated thermal efficiency of the naturally aspirated baseline engine


© SAE International and SAE Naples Section.

Dealing with gross IMEP, also the gross indicated efficiency η_{ig} may be involved:

$$\eta_{ig} = \frac{IMEP_g \cdot \alpha}{\delta_0 \cdot \lambda_v \cdot LHV} = \eta_i \cdot \frac{IMEP_g}{IMEP} \quad (18)$$

whose values are shown as function of MAP and mean piston speed in Figure 9.

Proposed Thermal Unit: Naturally Aspirated Version

As already mentioned, the main characteristic of the proposed thermal unit relies on the exhaust energy recovery implemented by means of a suitable expander (E) connected to its dedicated electric generator (G_E), as shown in Figure 2. Differently from common turbocharged engine, in the system proposed the expander is exclusively dedicated to complete the exhaust gas expansion. To this purpose, in the system proposed, the engine exhaust pressure (p_e) will be necessarily

higher than in the case of the baseline engine (p_{s0}), which was supposed to be slightly higher than the ambient pressure p_0 (i.e. $p_{s0} \approx 1.06 p_0$). As obvious, the energy recovered by the expander-generator increases with the exhaust pressure p_s , and hence with the expander pressure ratio $\beta_s = p_s/p_{s0}$. On the other hand, as known, the increase of the exhaust pressure influences both the indicated and the volumetric efficiency of the engine. A higher exhaust pressure will in effect increase the amount of in-cylinder residual gas, thus lowering the entrapped mass of fresh charge. Moreover, as is known, diluting fresh charge with residual gas decreases both flame propagation speed and combustion efficiency, thus compromising the engine indicated efficiency. In the calculation performed, both effects were taken into consideration. The approach here followed by the authors represents another original aspect with respect to [17], where the variation of the indicated efficiency was neglected. As regards the volumetric efficiency, a correction factor usually employed to account for the effect of pressure difference between inlet and exhaust on the volumetric efficiency is:

$$\lambda'_V(n) = 1 + \frac{MAP - p_s}{k \cdot MAP \cdot (\rho - 1)} \quad (19)$$

This correction factor is obviously 1 when no pressure difference exists between inlet and exhaust, and decreases when the exhaust backpressure is higher than MAP. Since the baseline engine was considered to discharge at the exhaust pressure p_{s0} , with the aim to account for the variation of the inlet to exhaust pressure difference due to p_s variation, the authors considered that, for each mean piston speed, the correction factor to adopt for any MAP or p_s variation is:

$$\lambda_V(u_m) = \frac{1 + \frac{MAP - p_s}{k \cdot MAP \cdot (\rho - 1)}}{1 + \frac{p_0 - p_{s0}}{k \cdot p_0 \cdot (\rho - 1)}} \quad (20)$$

being λ_{V0} the volumetric efficiency of the baseline engine corresponding to the manifold pressure p_0 and the exhaust pressure p_{s0} (considered = $1.06 p_0$), for a given mean piston speed u_m . As a final result, the volumetric efficiency of the engine running with any MAP or p_s values can be evaluated employing equation (20):

$$\lambda_V(u_m) = \lambda_{V0}(u_m) \cdot \left[\frac{1 + \frac{MAP - p_s}{k \cdot MAP \cdot (\rho - 1)}}{1 + \frac{p_0 - p_{s0}}{k \cdot p_0 \cdot (\rho - 1)}} \right] \quad (21)$$

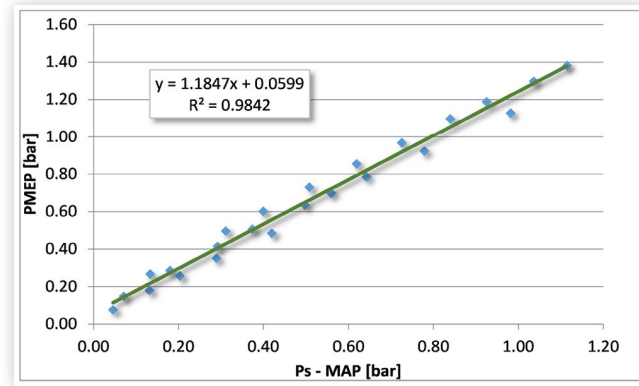
As regards the second effect related to the increase of the exhaust pressure, i.e. the worsening of the indicated efficiency, the authors could not trace any valid reference in the literature. Given this lack of information, the authors carried out a special series of experimental tests, with the aim to correlate the indicated efficiency deterioration in a spark ignition engine as a function of the in-cylinder residual gas fraction (RGF); to the purpose, a pressure throttling valve was installed in the exhaust duct of the engine used for the test (a four cylinder 1.2 L multi point spark ignition engine fuelled with CNG); the in-cylinder pressure was measured by means of a

TABLE 4 Operative conditions of the experimental test

Engine speed [rpm]	1500-2500-3500
Throttle position	Wide open
MAP [bar]	1.00
Exhaust pressure p_s [bar]	1.0 to 2.0 in steps of 0.1
Fuel	CNG
Spark advance	Optimal (LPP=15°ATDC)
Air-fuel ratio	Stoichiometric

© SAE International and SAE Naples Section.

FIGURE 10 PMEP increment due to the exhaust pressure increase



© SAE International and SAE Naples Section.

flush mounted AVL GU13X piezoelectric pressure sensor, and sampled with the resolution of 1 CAD using a 360 ppr optical encoder connected to the engine crankshaft; air and fuel mass flow were also recorded, together with manifold absolute pressure and engine torque. A more detailed description of the engine test bed is reported in [19, 20]. The operative conditions of the test performed are resumed in Table 4: for each engine speed, the exhaust pressure was increased from 1 bar (no exhaust gas throttling) in steps of 0.1 bar until heavy combustion instability, without exceeding to 2 bar.

As shown in Figure 10 and Figure 11, the results of these experimental tests confirmed that increasing the exhaust pressure with constant MAP reduces the IMEP of the engine for two different reason: one is related to the pumping cycle (Figure 10), whose area increases and causes a reduction of the net IMEP, while the second is instead related to the fresh charge dilution with residual gas, which determines a reduction of the gross indicated thermal efficiency (Figure 11).

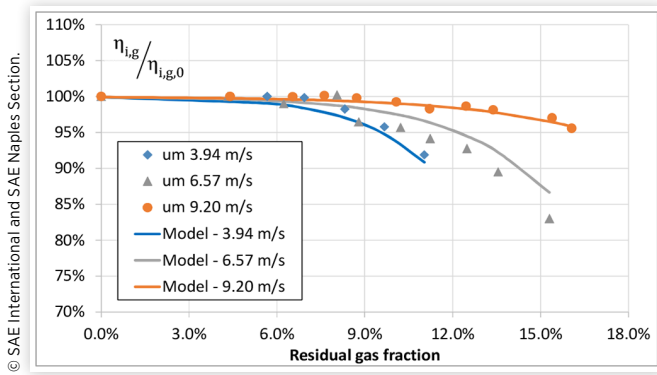
As a result, it was obtained that, to account for the effect of exhaust pressure increase, a two steps calculation is required; first, the pumping mean effective pressure (PMEP) must be evaluated as function of the pressure difference (p_s -MAP) according to the linear relation shown in Figure 10:

$$PMEP_{[bar]} = 1.185 \cdot (p_{s[bar]} - MAP_{[bar]}) + 0.06 \quad (22)$$

In the second calculation step, instead, the variation of the gross indicated efficiency ($\eta_{i,g}$) is obtained as function of the residual gas fraction RGF:

$$\eta_{i,g} = \frac{1}{1 + e^{(-7.15 - \gamma \cdot RGF)}} \quad (23)$$

FIGURE 11 Gross IMEP variation due as function of the RGF change



Where $\eta_{i,g,0}$ represents the reference gross indicated efficiency of the engine (i.e. without throttling the exhaust duct), while the speed parameter γ is related to the engine mean piston speed u_m , which, as shown by the experimental data, has a strong influence on the variation of the efficiency:

$$\gamma = 3.61 \cdot u_m - 58.22 \quad (24)$$

The residual gas fraction RGF is the ratio between the residual gas mass and the fresh charge mass, whose calculation procedure is reported in the Appendix. The performances of the engine in the proposed thermal unit were evaluated starting from the baseline engine according to the assumption that the same technology level shall be employed, and hence the same specific performance would be obtained, unless modification or parameters variations occur.

For each MAP (from 0.3 bar to 1 bar) and mean piston speed (from 2 to 17 m/s), the gross indicated efficiency $\eta_{i,g}$ of the engine in the thermal unit can be evaluated by means of equations (23) and (24) starting from the gross indicated efficiency $\eta_{i,g,0}$ of the baseline naturally aspirated engine at the same MAP and mean piston speed u_m , and once the residual gas fraction is determined. The gross $IMEP$ is hence derived from equation (18):

$$IMEP_g = \frac{\delta_0 \cdot \lambda_V \cdot LHV \cdot \eta_{ig}}{\alpha} \quad (25)$$

while the net $IMEP$ is derived by means of equation (22):

$$IMEP = IMEP_g - PMEP \quad (26)$$

Using the same $FMEP$ model employed for the baseline engine, the $BMEP$ of the engine in the thermal unit can be then calculated for each MAP and mean piston speed:

$$BMEP = IMEP - FMEP \quad (27)$$

The overall specific output $BMEP_{TOT}$ of the proposed thermal unit is composed by the engine $BMEP$ and by the specific output of the expander-generator group, i.e. the recovery mean equivalent pressure $RMEP$:

$$BMEP_{tot} = BMEP + RMEP \quad (28)$$

Where the recovery mean effective pressure is evaluated on the basis of the power recovered by the expander-generator group P_{exp} :

$$RMEP = \frac{60 \cdot \varepsilon \cdot P_{exp}}{V_{AX} \cdot n} \quad (29)$$

Here V_{AX} represents displacement of the engine of the proposed thermal unit, while ε is the number of revolutions per cycle, which, for a 4 stroke engine, is 2. The power P_{exp} produced by the expander-generator group is evaluated as:

$$P_{exp} = G_0 \cdot \frac{\alpha + 1}{\alpha} \cdot c_{p,s} \cdot \eta_E \cdot T_S \cdot \left(1 - \beta_S^{\frac{1-k_S}{k_S}} \right) \quad (30)$$

where G_0 is the air mass flow of the engine, α is the air-fuel ratio, T_S the exhaust gas temperature at the expander inlet, η_E the expander efficiency (here supposed constant = 0.75), $\beta_S = p_s/p_{s0}$ is the pressure ratio across the expander and k_S the isentropic coefficient of the exhaust gas. As can be noted by equation (29) and (30), the efficiency of the generator G_E is not considered in the power obtained by exhaust gas expansion. This is not an unfair evaluation, but coherently follows the evaluation performed on the power produced by the engine, which was not reduced by the efficiency of the connected electrical machine of the generic hybrid propulsion system which should employ the baseline engine or the proposed thermal unit.

A simple correlation developed for the evaluation of the exhaust gas temperature T_S was employed

$$T_S = T_1 \cdot \frac{p_s}{MAP} \cdot \frac{(k_S - 1)}{k_S} + \frac{T_4}{T_1} \cdot \frac{1}{k_S} \quad (31)$$

where the T_1 represent the inlet temperature at intake valve closure (IVC), which is roughly the ambient temperature T_0 , while T_4 is the in-cylinder gas temperature at the exhaust valve opening (EVO). According to experimental findings and confirmed by data reported in the scientific literature, for a spark ignition engine the ratio T_4/T_1 ranges from 3.5 to 4.5: in the calculation performed it was hence considered constant = 4.

The isentropic coefficient k_S of the exhaust gas was computed as the ratio between the constant pressure and the constant volume specific heats of the burned gas, both evaluated at the exhaust gas temperature T_S :

$$k_S = \frac{c_{p,s}(T_S)}{c_{v,s}(T_S)} \quad c_{v,s}(T_S) = c_{p,s}(T_S) - R_S' \quad (32)$$

where both $c_{p,s}$ and R_S' were calculated as weighted average on the basis of the burned gas composition:

$$c_{p,s} = c_{p,CO_2}(T_S) \cdot x_{CO_2} + c_{p,H_2O}(T_S) \cdot x_{H_2O} + c_{p,N_2}(T_S) \cdot x_{N_2} + c_{p,CO}(T_S) \cdot x_{CO} \quad (33)$$

$$R_S' = R'_{CO_2} \cdot x_{CO_2} + R'_{H_2O} \cdot x_{H_2O} + R'_{N_2} \cdot x_{N_2} + R'_{CO} \cdot x_{CO} \quad (34)$$

being x the mass fraction of the generic chemical species: to this purpose, the combustion of C_8H_{18} was considered for the calculation of each species mass concentration. It is worth noting that the last terms of both equations (33) and (34) refer to the presence of carbon monoxide, which has been considered only when rich air-fuel mixtures were adopted. The specific heat at constant pressure of each chemical species was calculated as function of the exhaust gas temperature T_S by

means of the Shomate equations and coefficients available at the NIST Chemistry WebBook [21]. The calculation procedure here described and followed by the authors constitutes a further point of difference with respect to [17], where the gas has been assumed to be ideal, i.e. with constant specific heats, and without any difference between burned and unburned.

The engine air mass flow G_O is:

$$G_O = \frac{V_{AX} \cdot n}{60 \cdot \varepsilon} \cdot \delta_0 \cdot \lambda_V \quad (35)$$

where λ_V is the engine volumetric efficiency determined in equation (21), δ_0 the air density in the manifold, n the engine speed.

Substituting equations (30) and (35) into equation (29), the recovery mean effective pressure is obtained:

$$RMEP = \delta_0 \cdot c_{p,s} \cdot \lambda_V \cdot \frac{\alpha + 1}{\alpha} \cdot \eta_E \cdot T_s \cdot \left(1 - \beta_S^{\frac{1-k_s}{k_s}} \right) \quad (36)$$

The overall specific output of the thermal unit $BMEP_{TOT}$ can be hence calculated from equation (28); as final calculation, the overall brake thermal efficiency $\eta_{b,TOT}$ (and the consequent overall brake specific fuel consumption $BSFC_{TOT}$) of the proposed thermal unit can be evaluated:

$$\eta_{b,TOT} = \frac{BMEP_{TOT} \cdot \alpha}{\delta_0 \cdot \lambda_V \cdot LHV} \quad (37)$$

$$BSFC_{TOT} \text{ [g/kWh]} = \frac{3600}{LHV_{[MJ/kg]} \cdot \eta_{b,TOT}} \quad (38)$$

It is worth pointing out that the overall efficiency determined by equation (37) does not refer to the internal combustion engine only, but rather to the entire thermal unit, composed by the engine and the expander-generator. The overall output power is hence:

$$P_{TOT} = BMEP_{TOT} \cdot \frac{V_{AX} \cdot n}{60 \cdot \varepsilon} \quad (39)$$

For each operative condition of MAP and mean piston speed u_m , the authors evaluated the optimal value of the exhaust pressure p_s maximizing the overall brake thermal efficiency $\eta_{b,TOT}$. The resulting optimized values of the exhaust pressure as a function of speed and load are shown in Figure 12. It is worth pointing out that the control of the exhaust pressure would be referred to the electronic control unit of the thermal unit, which should be programmed to properly manage the electric generator connected to the expander.

Once optimized each operation point of the proposed thermal unit, the maximum $BMEP_{TOT}$ was determined to be 11.3 bar (slightly lower with respect to the baseline engine), thus allowing to establish the engine displacement V_{AX} required to obtain the predetermined output power of 73.5 kW: $V_{AX} = 1636 \text{ cc}$. The overall brake specific fuel consumption $BSFC_{tot}$ of the proposed thermal unit, calculated from equations (37) and (38), is hence reported in Figure 13. Employing the same parameters adopted for the baseline engine (bore/stroke ratio, volumetric compression ratio, and maximum cylinder displacement) the main characteristics of the thermal unit were determined, as reported in Table 5 together with some performance results. As first observation, it can be noted that the minimum brake specific fuel consumption slightly

FIGURE 12 Optimal exhaust pressure p_s [bar] as a function of speed and load for the proposed thermal unit

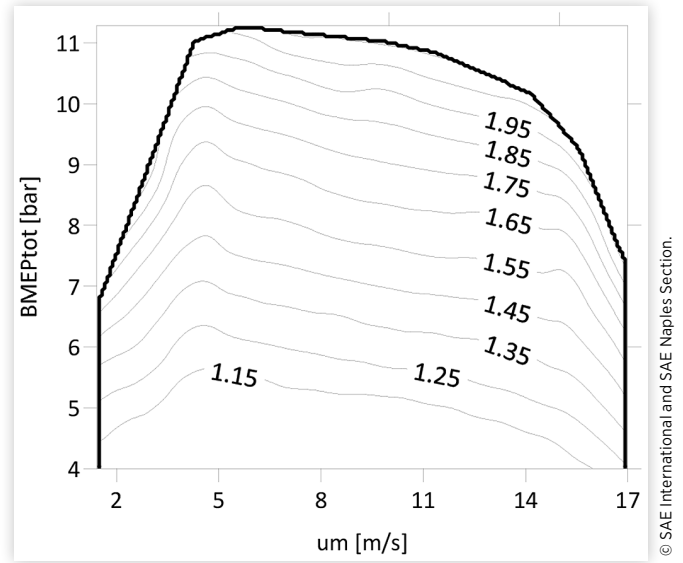
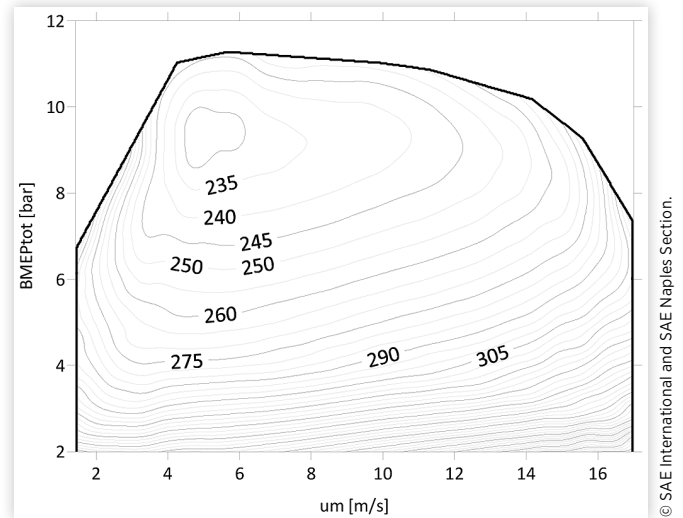


FIGURE 13 Fuel consumption of the naturally aspirated thermal unit [g/kWh]



decreased from 236.9 g/kWh of the baseline naturally aspirated engine to 231.9 g/kWh of the new thermal unit. As regards the expander participation to the overall power output, it can be noted that the recovery mean equivalent pressure reached the maximum value of 1.72 bar (being 9.66 bar the maximum BMEP expressed by the engine), with a maximum share of power produced of 17.2%.

Considering, as already mentioned, the application of the proposed thermal unit on a hybrid electric vehicles, the efficiency comparison with respect to the baseline engine was carried out on the same output power level; to this purpose Figure 14 reports the efficiency increments obtained with respect to the baseline engine. As can be noted, the energetic advantages connected to the implementation of the proposed thermal unit are positive only for power output higher than 20 kW, and assume significant values in the upper load region, where the higher in-cylinder pressure produces better recovery

TABLE 5 Main characteristic of the naturally aspirated thermal unit

Engine	4-stroke, naturally aspirated spark ignition
Displacement	1636 cc
Number of Cylinders	4
Bore	80.4 mm
Stroke	80.4 mm
Compression Ratio	11
Injection system	Gasoline direct injection
Valvetrain	4 valves/cylinder, VVT
Expander efficiency	0.75
Max overall output Power	73.5 kW at 5800 rpm
Max BMEP _{TOT}	11.3 bar at 2100 rpm
Min BSFC _{tot}	231.9 g/kWh
Max Engine BMEP	9.66 bar at 2100 rpm
Max Expander RMEP	1.72 bar at 3700 rpm
Max RMEP/BMEP _{TOT}	17.2%

© SAE International and SAE Naples Section.

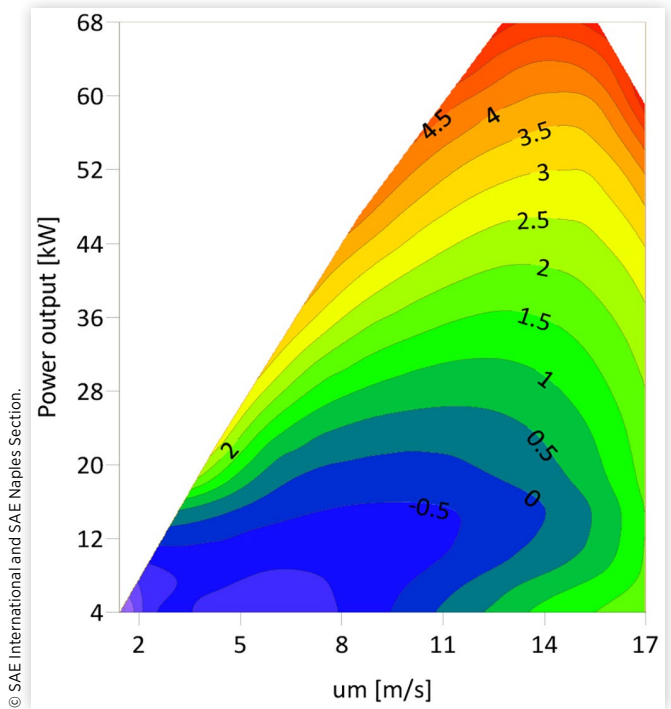
conditions for the expander. Although low performance improvements were found (efficiency increments higher than 5% are obtained only for power output above 60 kW), the suitability of the thermal unit may improve when the vehicle usage in urban and in extra-urban area is concerned: to this purpose, the authors plan on improving the model accuracy and reliability with the aim to perform simulations involving the application on official driving cycles.

Baseline Turbocharged Engine

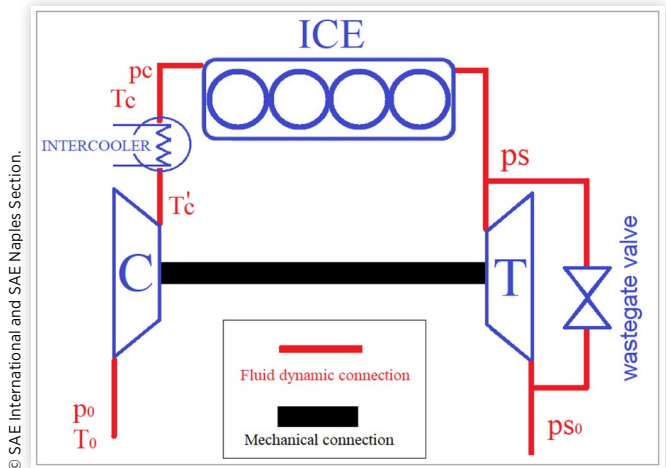
As already mentioned, the comparison of the evaluation of the performance increment obtained by the proposed thermal unit was carried out both with a naturally aspirated and a supercharged engine. In this section the authors develop the calculations for the determination of the baseline turbocharged engine, which will be compared to the supercharged version of the proposed thermal unit. As stated before, all the engines and thermal units were compared on the same output power basis, i.e. each engine was sized to obtain the same maximum power of 73.5 kW. To this purpose, the engine size is determined once the specific performance, i.e. BMEP, is known.

The evaluation of the turbocharged engine BMEP is performed starting from the parameters and specific performance of the baseline naturally aspirated engine. Figure 15 reports the schematic representation of the turbocharged engine here considered: the turbocharger is composed by the turbine T and the compressor C, which are both fluid-dynamically connected to the engine. The system comprises an inter-cooler for charge cooling and a waste-gate valve for the turbine by-pass when the compression ratio tends to exceed the maximum allowed boost pressure, here assumed to be 1.5 bar.

For the evaluation of the specific performance of the turbocharged engine, it must be considered that, for each MAP and mean piston speed u_m , the air mass flow to the engine is:

FIGURE 14 Efficiency improvement [%] of the thermal unit with respect to the baseline engine (both naturally aspirated)


© SAE International and SAE Naples Section.

FIGURE 15 Scheme adopted of the turbocharged baseline engine


© SAE International and SAE Naples Section.

$$G_C = \frac{V_T \cdot n}{60 \cdot \varepsilon} \cdot \delta_C \cdot \lambda_{vC} \quad (40)$$

where V_T is the displacement of the turbocharged engine, n is the engine speed, while δ_C and λ_{vC} represent the air density in the manifold and the volumetric efficiency of the turbocharged engine respectively. The air density is:

$$\delta_C = \frac{MAP}{R' \cdot T_C} \quad (41)$$

given by the manifold absolute pressure MAP and by the outlet temperature from the intercooler T_C . It is worth noting that

the MAP values may result lower than the compressor outlet pressure p_c due to the throttling made for the lower part load operation. The outlet temperature from the intercooler can be estimated assuming the intercooler efficiency R_{INT} equal to 0.7, hence:

$$T'_C = T_0 \cdot \left(1 + \frac{\beta_C^{\frac{k-1}{k}} - 1}{\eta_C} \right) \quad (42)$$

$$T_C = T'_C - R_{INT}(T'_C - T_0) \quad (43)$$

being T'_C the outlet temperature from the compressor, evaluated in [equation \(42\)](#) by means of the compression ratio $\beta_C = p_c/p_0$ and of the compressor efficiency η_C (here assumed constant = 0.65). On account of the higher temperatures in the engine manifold induced by the compressor, the authors considered the typical reduction of the engine volumetric compression ratio ρ with respect to the naturally aspirated engine, in line with the guidelines usually followed to avoid dangerous knocking phenomena in turbocharged or supercharged engine. The necessary reduction of the engine compression ratio was based on considerations and data traceable in the literature and on the most recent strategies adopted in spark ignition engines. Starting from the compression ratio of 11 adopted for the naturally aspirated gasoline engine, and considering a maximum boost pressure of 1.5 bar, the compression ratio of the turbocharged engine ρ' could be plausibly assumed to be 10.

The volumetric efficiency λ_{VC} of the turbocharged engine is evaluated on the basis of the volumetric efficiency of the naturally aspirated engine λ_{V0} as function of the mean piston speed u_m with two corrections: one is related to the increased inlet temperature (which, as known, increase the volumetric efficiency), while the other is due to the inlet to exhaust pressure difference (see equations from (19) to (21)), which, in the turbocharged engine is different from the naturally aspirated.

$$\lambda_{VC}(u_m) = \lambda_{V0}(u_m) \cdot \sqrt{\frac{T_C}{T_0}} \cdot \left[\frac{1 + \frac{MAP - p_s}{k \cdot MAP \cdot (\rho' - 1)}}{1 + \frac{p_0 - p_{s0}}{k \cdot p_0 \cdot (\rho - 1)}} \right] \quad (44)$$

It must be observed that the same maximum mean piston speed $u_{m,max}$ of the naturally aspirated engine (see [Table 1](#)) is assumed for all the engine compared in this study, according to the assumption that the same technology level is shared among the different engines, and hence the same mechanical performance can be obtained.

The air mass flow G_C to the engine is delivered by the compressor, whose required power P_{comp} is supplied by the turbine, whose power output is P_{turb} . The power balance is hence:

$$\begin{aligned} P_{comp} &= G_C \cdot c_{pC} \cdot \frac{T_0}{\eta_C} \cdot \left(\beta_C^{\frac{k-1}{k}} - 1 \right) \\ &= P_{turb} = G_T \cdot c_{pS} \cdot \eta_t \cdot T_S \cdot \left(1 - \beta_S^{\frac{1-k_s}{k_s}} \right) \end{aligned} \quad (45)$$

where G_T is the gas mass flow in the turbine, T_S is the exhaust gas temperature at the pressure p_s , c_{pC} and c_{pS} are the constant pressure specific heat of the fresh air and exhaust gas respectively, η_t is the turbine efficiency (here assumed constant = 0.55), and $\beta_S = p_s/p_{s0}$ is the pressure ratio across the turbine. The gas mass flow in the turbine G_T is linked to the compressor mass flow G_C by the relation:

$$G_T = \Omega \cdot G_C \frac{\alpha + 1}{\alpha} \quad (46)$$

where the correction $[(\alpha + 1)/\alpha]$ accounts for the fuel mass flow added in the engine, while Ω represents the fraction of exhaust gas mass flow which runs through the turbine, being the rest by-passed by the waste-gate valve whenever the boosting pressure p_c tends to exceeds the predetermined limit (usually is $0.4 \leq \Omega \leq 1$). From the power balance of [equation \(45\)](#) it derives that the turbocharging compression ratio is:

$$\beta_C = \left[1 + \Omega \cdot \frac{\alpha + 1}{\alpha} \cdot \frac{c_{pS}}{c_{pC}} \cdot \frac{T_S}{T_0} \cdot \eta_t \cdot \eta_C \cdot \left(1 - \frac{1}{\beta_S^{\frac{k_s-1}{k_s}}} \right) \right]^{\frac{k_c}{k_c-1}} \quad (47)$$

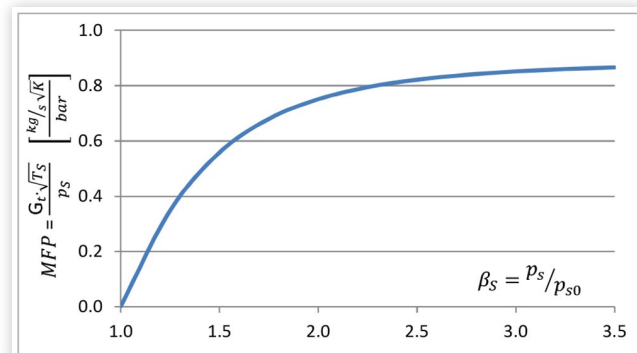
In the calculation performed, whenever β_C tends to exceeds the limit value (i.e. 1.5), the parameter Ω is reduced (which corresponds to the waste-gate opening) until the limit is respected. The exhaust gas temperature can be evaluated by means of the equation already mentioned:

$$T_S = T_C \cdot \frac{p_S}{MAP} \cdot \frac{(k_s - 1)}{k_s} + \frac{T_{4,C}}{T_C} \cdot \frac{1}{k_s} \quad (48)$$

where k_s is the isentropic coefficient of the exhaust gas, whose calculation, together with c_{pS} , has been already discussed in [equations \(32\)](#) [\(33\)](#) and [\(34\)](#). The ratio $T_{4,C}/T_C$, as before, is considered constant = 4.

The system of equation used to describe the turbocharger power and mass flow balance is completed by the turbine characteristic curve, which account for the limited swallowing capacity of the turbine and correlates its pressure drop to the mass flow. As shown in [Figure 16](#), a simplified representation was adopted, where one single curve describes the mass flow parameter (MFP) of the turbine instead of multiple curves at different speeds of rotation.

FIGURE 16 Performance characteristic of the turbine considered (Mass flow parameter vs pressure ratio)



Since the MFP correlates the turbine mass flow to inlet turbine condition of pressure and temperature:

$$MFP = \frac{G_T \cdot \sqrt{T_s}}{p_s} \quad (49)$$

with the aim to evaluate the MFP from β_s (and vice-versa), the authors adopted a suitable mathematical expression which faithfully reproduces the typical progress of the MFP as function of the pressure ratio β_s :

$$MFP = \frac{a \cdot b + c \cdot \beta_s^d}{b + \beta_s^d} \quad (50)$$

where the constants a , b , c and d were obtained by means of data fitting performed on the characteristic of a market available product. As a final step, the MFP values deriving from equation (49) have been amplified (or reduced) to virtually adapt the turbine size to the engine size and parameters resulting from calculations.

The calculation of the turbocharger performance requires the recursive solution of the system of equations from (42) to (49) for each MAP (from 0.4 bar up to the maximum allowed value of 1.5 bar) and mean piston speed u_m (from 2 to 17 m/s). Once reached the solution, the condition of the gas at both inlet and outlet of the engine are determined and the performance of the engine may be evaluated. To this purpose the authors made a simplifying assumption based on the consideration that two similar engines, with same technological development level, both running at full load (or wide open throttle, WOT) and at the same mean piston speed, but with different manifold absolute pressures, will deliver different powers with almost the same efficiency. According to this assumption the gross indicated efficiency of the turbocharged engine has been evaluated on the basis of the gross indicated efficiency of the naturally aspirated engine for the same mean piston speed and same normalized MAP value, and corrected for the different engine compression ratio. Hence, defining:

$$\phi = \frac{MAP}{MAP_{max}} \quad (51)$$

the simplifying assumption implies that:

$$\eta_{ig,C}(\phi, u_m) = \eta_{ig}(\phi, u_m) \cdot f_{CR} \quad (52)$$

where f_{CR} is a correction factor which takes into account the different compression ratio of the turbocharged engine with respect to the naturally aspirated. According to the basic theory of the ideal Otto cycle, the correction factor f_{CR} was computed as the ratio of the ideal efficiency of the two Otto cycles with different compression ratio:

$$f_{CR} = \frac{\eta_{Otto}'}{\eta_{Otto}} = \frac{1 - \frac{1}{\rho'^{k-1}}}{1 - \frac{1}{\rho^{k-1}}} \quad (53)$$

The gross indicated mean effective pressure of the turbocharged engine is hence evaluated as:

$$IMEP_{g,C} = \frac{\delta_C \cdot \lambda_{v,C} \cdot LHV}{\alpha} \cdot \eta_{ig,C} \quad (54)$$

and hence the net indicated mean effective pressure:

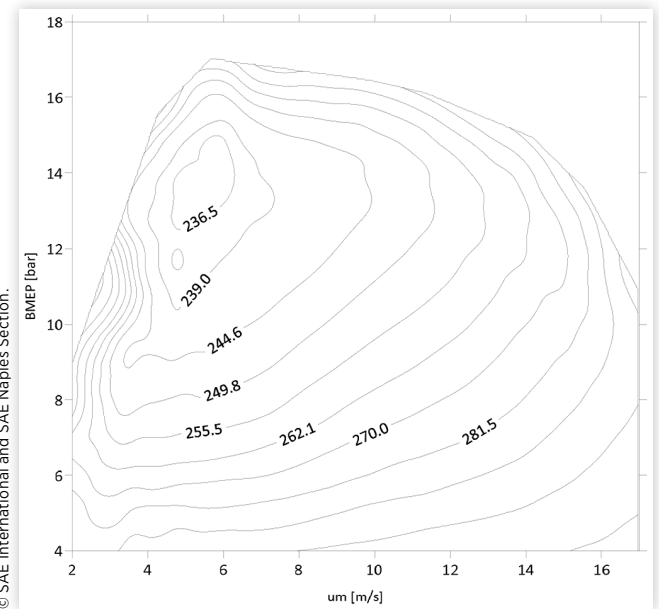
$$IMEP_C = IMEP_{g,C} + PMEP_C \quad (55)$$

TABLE 6 Main characteristics of the turbocharged engine

Engine	4-stroke, Turbocharged Spark Ignition
Displacement	1074 cc
Number of Cylinders	3
Bore	77.0 mm
Stroke	77.0 mm
Compression Ratio	10
Injection system	Gasoline direct injection
Valvetrain	4 valves/cylinder, VVT
Max BMEP _C	17.0 bar 2200 rpm
Max Power	73.5 kW at 5500 rpm
Min BSFC	236.3 g/kWh
Max Boost pressure	1.5 bar

© SAE International and SAE Naples Section.

FIGURE 17 Brake specific fuel consumption of the turbocharged engine [g/kWh]



© SAE International and SAE Naples Section.

being the mean pumping mean effective pressure $PMEP_C$ evaluated by means of equation (22). The friction mean effective pressure may still be evaluated by the same equation (9) used for the naturally aspirated engine, hence the brake mean effective pressure $BMEP_C$ of the turbocharged engine can be finally calculated together with the related brake specific fuel consumption $BSFC_C$:

$$BMEP_C = IMEP_C + FMPEP_C \quad (56)$$

$$BSFC_C = \frac{\delta_C \cdot \lambda_{v,C}}{BMEP_C \cdot \alpha} \quad (57)$$

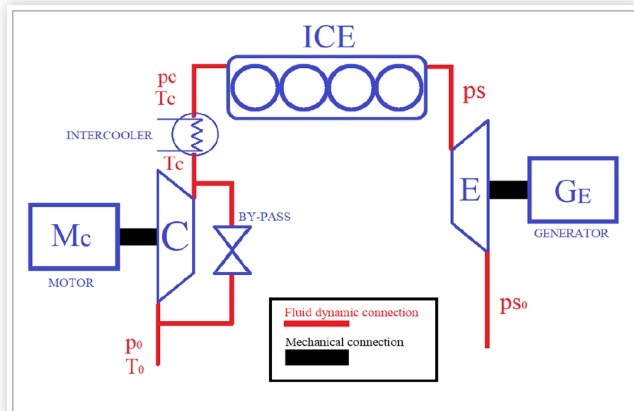
Given the required output power of 73.5 kW, on the basis of the maximum $BMEP_C$ obtained by the turbocharged engine (17.0 bar), the necessary displacement V_T resulted 1074cc., which, with the same consideration made for the naturally aspirated engine, can be subdivided into 3 cylinders with bore/stroke ratio = 1. The main characteristics and performance of the baseline turbocharged engine are resumed in Table 6.

Supercharged Version of the Proposed Thermal Unit:

In this section the performance of the proposed thermal unit in the supercharged version will be evaluated and compared to the performance of the traditional turbocharged engine. As already mentioned, the baseline naturally aspirated engine represents the starting point of this evaluation, and the comparison will be carried out on an equal power basis. [Figure 18](#) reports the schematic representation of the system proposed: as can be seen, the thermal unit is composed by a supercharged engine, whose exhaust gas complete their expansion on a dedicated expander, quite like in the naturally aspirated version. The main difference with respect to the turbocharged engine is that the compressor is not mechanically connected to the expander, but is powered by means of an electric motor, which is supplied by the same energy storage system which receives the power produced by the expander-generator (e.g. the batteries of an hybrid propulsion system). It is also assumed that the control system regulates the compressor speed of rotation so as to increase the air pressure only when needed, that is when MAP values higher than 1 bar are required, thus reducing its power absorption when the engine load is low ($MAP < 1$ bar): as shown in [Figure 18](#), a by-pass valve is used to let the air flow in this condition. As already mentioned, the expander is always active, thus permanently recover as much energy as possible from the exhaust gas.

As in the case of the turbocharged engine, the efficiency of both compressor ($\eta_C = 0.65$) and expander ($\eta_E = 0.75$) were supposed to remain constants for all the engine operative conditions. Moreover, as mentioned in the case of the naturally aspirated thermal unit, the efficiency of the expander is assumed higher than in a common turbine since it is considered an optimized machine, working in quasi-steady state condition, dedicated to the energy production and not to compressor moving. Also the engine compression ratio was supposed decreased to 10 as in the turbocharged case. This will be taken into consideration in the estimation of the indicated thermal efficiency.

FIGURE 18 Schematic representation of the proposed supercharged thermal unit



© SAE International and SAE Naples Section.

For the evaluation of the performance of the supercharged thermal unit, the same MAP values (from 0.4 bar to the maximum allowed 1.5 bar) and mean piston speed u_m (from 2 to 17 m/s) of the turbocharged engine were considered. The gross indicated mean effective pressure $IMEP_{g,C}$ was evaluated by means of the same assumption made for the turbocharged engine, i.e. using [equations \(51\) \(52\)](#) and [\(53\)](#):

$$IMEP_{g,C} = \frac{\delta_C \cdot \lambda_{V,C} \cdot LHV}{\alpha} \cdot \eta_{ig,C} \quad (58)$$

where δ_C is evaluated as in [equation \(41\)\(42\)](#) and [\(43\)](#). As already mentioned for the naturally aspirated thermal unit, a higher exhaust pressure p_s produces a reduction in the engine volumetric efficiency $\lambda_{V,C}(u_m)$, evaluated by means of [equation \(44\)](#), and in the gross indicated efficiency, evaluated by means of [equations \(23\)](#) and [\(24\)](#) starting from the reference gross indicated efficiency $\eta_{i,g,0}$ of the turbocharged engine at the same MAP and mean piston speed u_m . The net indicated mean effective pressure $IMEP_C$ is hence calculated as:

$$IMEP = IMEP_g - PMEP \quad (59)$$

where the pumping mean effective pressure is obtained by [equation \(22\)](#). [Equation \(9\)](#) is employed to evaluate the $FMEP_C$, and hence the $BMEP_C$ is obtained. To determine the overall $BMEP_{tot}$ of the supercharged thermal unit, the expander $RMEP$ must be added, while the compression mean equivalent pressure $CMEP$ must be subtracted:

$$BMEP_{TOT} = BMEP + RMEP - CMEP \quad (60)$$

The $RMEP$ is obtained again as:

$$RMEP = \delta_C \cdot c_{p,s} \cdot \lambda_{V,C} \cdot \frac{\alpha + 1}{\alpha} \cdot \eta_E \cdot T_s \cdot \left(1 - \beta_s^{\frac{1-k_s}{k_s}} \right) \quad (61)$$

being T_s the exhaust gas temperature at the expander inlet, evaluated by [equation \(47\)](#), η_E the expander efficiency and $\beta_s = p_s/p_{s0}$ the pressure ratio across the expander.

The $CMEP$ is calculated on the basis of the power required by the compressor:

$$CMEP = \frac{60 \cdot \varepsilon \cdot P_{comp}}{V_{SX} \cdot n \cdot \eta_{EM}} \quad (62)$$

being V_{SX} the displacement of the supercharged engine in the thermal unit, and P_{comp} the power required by the compressor:

$$P_{comp} = G_C \cdot c_{p,c} \cdot \frac{T_0}{\eta_C} \cdot \left(\beta_c^{\frac{k_c-1}{k_c}} - 1 \right) \quad (63)$$

As can be noted, the efficiency of the electric motor was considered in the calculation of the $CMEP$, since it represents an ancillary device which burden on the energy balance of the engine. The engine air mass flow G_C is:

$$G_C = \frac{V_{SX} \cdot n}{60 \cdot \varepsilon} \cdot \delta_C \cdot \lambda_{VC} \quad (64)$$

being δ_C the air density in the manifold of [equation \(41\)](#). Substituting [equation \(41\)](#), [\(63\)](#) and [\(62\)](#) into [equation \(61\)](#), the $CMEP$ results:

$$CMEP = \frac{c_{p,c} \cdot T_0 \cdot \lambda_{VC} \cdot \delta_C}{\eta_{EM} \cdot \eta_C} \cdot \left(\beta_c^{\frac{k_c-1}{k_c}} - 1 \right) \quad (65)$$

For each operative condition of MAP and mean piston speed u_m , the authors evaluated the optimal value of the exhaust pressure p_s maximizing the overall brake thermal efficiency η_{bTOT} of the proposed thermal unit:

$$\eta_{bTOT} = \frac{BMEP_{TOT} \cdot \alpha}{\delta_C \cdot \lambda_{VC} \cdot LHV} = \frac{(BMEP + RMEP - CMEP) \cdot \alpha}{\delta_C \cdot \lambda_{VC} \cdot LHV} \quad (64)$$

The best efficiency values of the exhaust pressure as a function of speed and overall load are shown in [Figure 19](#), while the resulting overall brake specific fuel consumption $BSFC_{TOT}$ of the supercharged thermal unit is reported in [Figure 20](#):

$$BSFC_{TOT} = \frac{\delta_C \cdot \lambda_{VC}}{BMEP_{TOT} \cdot \alpha} \quad (66)$$

FIGURE 19 Optimal exhaust pressure levels [bar]

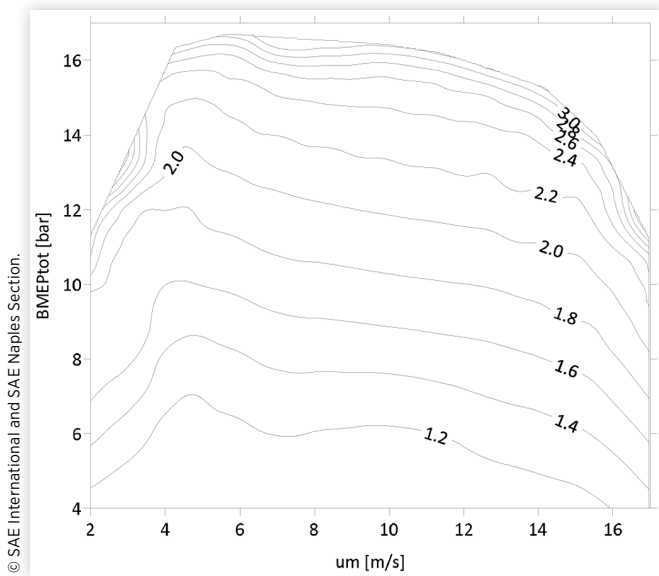
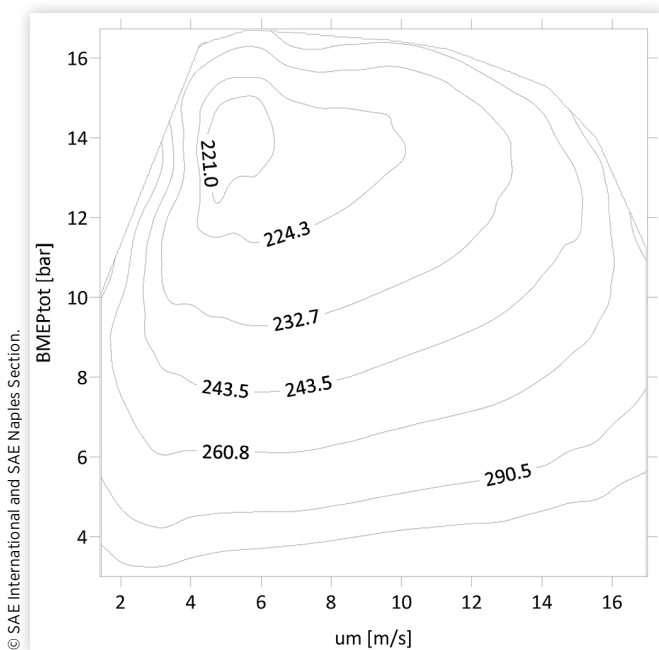


FIGURE 20 Overall brake specific fuel consumption of the supercharged thermal unit [g/kWh]



As can be noted, exhaust pressure as high as 3.2 bar were determined: this should be adequately considered for the study and development of a suitable high efficiency gas expander.

Once optimized the supercharged thermal unit, the maximum value of the $BMEP_{TOT}$ (16.72 bar, slightly lower than the turbocharged baseline engine) was employed for the determination of the engine displacement V_{SX} necessary to develop the target power of 73.5 kW: as resumed in [Table 7](#) together with some performance results, $V_{SX} = 1023$ cc. The displacement reduction of the supercharged version with respect to the naturally aspirated revealed quite similar to the downsizing obtained by turbocharging the baseline engine.

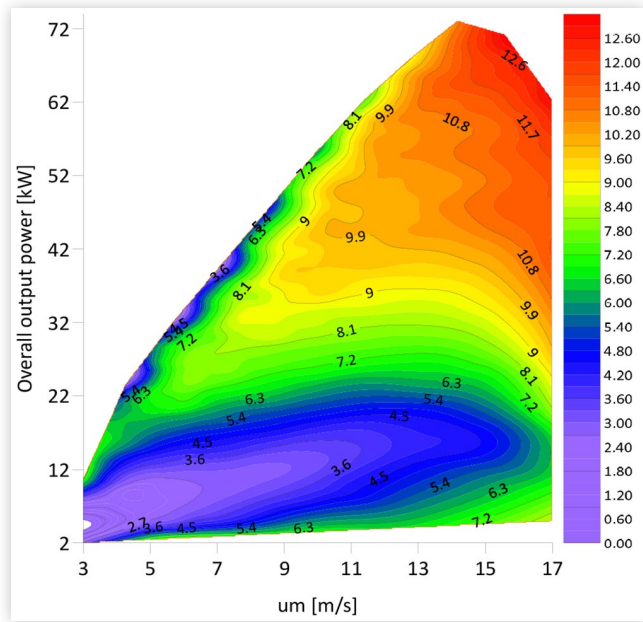
From the same [Table 7](#) it can be noted that the minimum overall specific fuel consumption of the supercharged thermal unit revealed 220.1 g/kWh which means a -6.9% with respect to the baseline turbocharged engine (236.3 g/kWh). [Table 7](#) also shows that the expander contributed to the overall $BMEP_{tot}$ with RMEP up to 3.9 bar and share of power produced up to 26.4%: the higher in-cylinder pressure due to supercharging granted a stronger participation of the expander; the availability of high efficiency expander-generator could allow bigger energy recovery and better overall fuel economy.

As in the case of the naturally aspirated version, the efficiency comparison with respect to the baseline turbocharged engine was performed on the same output power level; the results are reported in the diagram of [Figure 21](#); different observation can be made; first of all it must be observed that, contrary to the naturally aspirated case, only positive efficiency variations were obtained by the supercharged thermal unit, even in the lower power region. It can also be observed that, quite similar to the naturally aspirated case, the energetic advantage increases with the power levels, which, as already observed, can be explained considering that the higher are the in-cylinder pressure or the exhaust mass flow, the greater will be the contribution that the expander can bring to the power output without compromising the efficiency of the engine. More in detail, the maximum efficiency increments revealed around 12.6%. The authors consider these results encouraging because obtained on the basis of non-optimized elements: a proper study and optimization of the compound

TABLE 7 Main characteristic of the supercharged thermal unit

Engine	4-stroke, supercharged spark ignition
Displacement	1023 cc
Number of Cylinders	3
Bore	75.7 mm
Stroke	75.7 mm
Compression Ratio	10
Injection system	Gasoline direct injection
Valvetrain	4 valves/cylinder, VVT
Expander efficiency	0.75
Max overall output Power	73.5 kW at 6100rpm
Max $BMEP_{TOT}$	16.72 bar at 2200 rpm
Min $BSFC_{tot}$	220.1 g/kWh
Max Engine BMEP	13.84 bar at 2200 rpm
Max Expander RMEP	3.93 bar at 3900 rpm
Max RMEP/ $BMEP_{TOT}$	26.4%

FIGURE 21 Efficiency improvement (as function of power output and mean piston speed u_m) with respect to the traditional turbocharged engine



© SAE International and SAE Naples Section.

performance of both the engine and the expander could bring to better results.

Conclusion

In this paper the authors present a preliminary assessment of the energetic advantages obtainable by a thermal unit composed by a spark ignition engine endowed of an exhaust gas expander employed to totally recover the unexpanded gas energy typical of Otto and Diesel cycle. An electric generator connected to the expander is also considered for the conversion of the recovered energy into electrical energy: the proposed system is hence particularly suitable for hybrid electric vehicles, where the energy produced by the expander-generator could be stored in the energy storage system of the vehicle.

The assessment of the energetic benefit was performed by comparing the overall efficiency of the proposed thermal unit (considered both in the naturally aspirated and in the supercharged version) to the efficiency of a baseline reference engine with the same power output. The comparison was carried out only in steady state operative conditions, using simple yet effective calculations. With the aim to remain as close as possible to real engine efficiency, the calculations were performed making use of real engine performance data and values. Dealing with exhaust energy recovery by means of a gas expander, the authors also carefully took into account the effect of exhaust backpressure increase on the engine performance and efficiency: in particular, the effect on gross indicated efficiency, on pumping cycle and on the volumetric efficiency were properly modelled. For each operative condition, the optimal exhaust pressure value was obtained as best

compromise between engine and expander-generator performance, reaching hence the maximum overall efficiency of the thermal unit.

As a result, it was observed that, in the naturally aspirated version, the thermal unit obtained limited efficiency improvements (up to 5.5%) and only for overall output power higher than 20 kW. The contribution of the expander to the overall power delivered by the thermal unit arrived at 17.2%.

In the supercharged version, instead, the efficiency improvements obtained with respect to the traditional turbocharged engine were remarkably higher and positive for every output power level; more in detail, efficiency increment reached 12.6%, while the participation of the expander-generator to the overall power produced arrived to 26.4%. As could be expected, the efficiency improvements obtained by the thermal unit increased with the power level: this was explained by the author considering that the higher are the in-cylinder pressure or the exhaust mass flow, the greater will be the contribution that the expander can bring to the power output without compromising the efficiency of the engine.

As regards the expander boundary conditions, it was evaluated a maximum exhaust gas pressure of 3.2 bar, which should be adequately considered for an optimized design. Moreover, since the higher efficiency improvements were obtained in the high load-high speed region of the engine operative map, it follows that the exhaust gas temperature T_S at the expander inlet could reach 800–900°C: this may lead versus the adoption of a turbine (axial multi-stage or radial in-flow), considering that its development is already compliant with such temperatures (as for example in [15]).

References

1. European Commission, “COM (2011) 144 Final, WHITE PAPER, Roadmap to a Single European Transport Area - Towards a Competitive and Resource Efficient Transport System,” Brussels, Mar. 28, 2011.
2. European Commission, “Directorate-General for Communication, Citizens’ Information Union Policies: Transport,” https://europa.eu/european-union/topics/transport_en.
3. Pipitone, E., and Beccari, A., “A Study on the Use of Combustion Phase Indicators for MBT Spark Timing on a Bi-Fuel Engine,” SAE Technical Paper 2007-24-0051, 2007, <https://doi.org/10.4271/2007-24-0051>.
4. Aghaali, H., and Ångström, H.-E., “A Review of Turbocompounding as a Waste Heat Recovery System for Internal Combustion Engines,” *Renewable and Sustainable Energy Reviews* 49:813–824, 2015, doi:10.1016/j.rser.2015.04.144.
5. Noor, A.M., Puteh, R.C., and Rajoo, S., “Waste Heat Recovery Technologies in Turbocharged Automotive Engine - A Review,” *Journal of Modern Science and Technology* 2(1):108–119, 2014.
6. Alshammari, M., Alshammari, F., and Pesyridis, A., “Electric Boosting and Energy Recovery Systems for Engine Downsizing,” *Energies* 12(24):4636, 2019, doi:10.3390/en12244636.

7. Pasini, G., Lutzemberger, G., Frigo, S., Marelli, S. et al., "Evaluation of an Electric Turbo Compound System for SI Engines: A Numerical Approach," *Applied Energy* 162:527–540, 2016, doi:10.1016/j.apenergy.2015.10.143.
8. Arsie, I., Cricchio, A., Pianese, C., Ricciardi, V. et al., "Evaluation of CO₂ Reduction in SI Engines with Electric Turbo-Compound by Dynamic Powertrain Modelling," *IFAC-PapersOnLine* 28(15):93–100, 2015, doi:10.1016/j.ifacol.2015.10.014.
9. Millo, F., Mallamo, F., Pautasso, E., and Ganio Mego, G., "The Potential of Electric Exhaust Gas Turbocharging for HD Diesel Engines," SAE Technical Papers 2006-01-0437, 2006, doi:10.4271/2006-01-0437.
10. Hopmann, U., and Algrain, M., "Diesel Engine Electric Turbo Compound Technology," SAE Technical Paper 2003-01-2294, 2003, <https://doi.org/10.4271/2003-01-2294>.
11. Alias, M.N., Rosnizam, C.P., Srithar, R., Uday, M. et al., "Simulation Study on Electric Turbo-Compound (ETC) for Thermal Energy Recovery in Turbocharged Internal Combustion Engine," *Applied Mechanics and Materials* 799–800:895–901, 2015, doi:<https://doi.org/10.4028/www.scientific.net/AMM.799-800.895>.
12. Kant, M., Romagnoli, A., Mamat, A.M., and Martinez-Botas, R.F., "Heavy-duty Engine Electric Turbocompounding," *Proceedings of the Institution of Mechanical Engineers, Part D: Journal of Automobile Engineering* 229(4):457–472, 2015, doi:10.1177/0954407014547237.
13. Cipollone, R., Di Battista, D., and Gualtieri, A., "Turbo Compound Systems to Recover Energy in ICE," *International Journal of Engineering and Innovative Technology (IJEIT)* 3(6), 2013, <http://www.ijeit.com>.
14. Zhuge, W., Huang, L., Wei, W., Zhang, Y. et al., "Optimization of an Electric Turbo Compounding System for Gasoline Engine Exhaust Energy Recovery," SAE Technical Paper 2011-01-0377, 2011, <https://doi.org/10.4271/2011-01-0377>.
15. Haughton, A., and Dickinson, A., "Development of an Exhaust Driven Turbine-Generator Integrated Gas Energy Recovery System (TIGERS®)," SAE Technical Paper 2014-01-1873, 2014, doi:10.4271/2014-01-1873.
16. Abul Masrur, M., "Hybrid Electric Vehicles: Principles and Applications with Practical Perspectives," Chris Mi, San Diego State University, US, University of Detroit-Mercy, US.
17. Eriksson, L., Lindell, T., Leufven, O., and Thomasson, A., "Scalable Component-Based Modeling for Optimizing Engines with Supercharging, E-Boost and Turbocompound Concepts," *SAE Int. J. Engines* 5(2):579–595, 2012, <https://doi.org/10.4271/2012-01-0713>.
18. Cisotti, A., "Indagine sul rendimento organico dei motori ad accensione comandata di ultima generazione," Graduation thesis, Politecnico di Torino, 2001.
19. Pipitone, E. and Beccari, S., "Performance and Combustion Analysis of a Supercharged Double-Fuel Spark Ignition Engine," in *74th ATI National Congress, AIP Conf. Proc.*, vol. 2191, 020017-1-020017-9, 2019, <https://doi.org/10.1063/1.5138750>.
20. Pipitone, E., and Beccari, A., "A Study on the Use of Combustion Phase Indicators for MBT Spark Timing on a Bi-Fuel Engine," SAE Technical Paper 2007-24-0051, 2007, <https://doi.org/10.4271/2007-24-0051>.
21. NIST Chemistry WebBook, <https://webbook.nist.gov/chemistry/>.

Contact Information

Emiliano Pipitone,
University of Palermo,
emiliano.pipitone@unipa.it

Definitions/Abbreviations

BMEP - brake mean effective pressure [*bar*]
BMEP_{max} - maximum brake mean effective pressure [*bar*]
BMEP_{TOT} - Overall brake mean effective pressure of the thermal unit [*bar*]
BSFC - Brake specific fuel consumption [g/kWh]
BSFC_{TOT} - Overall BSFC of the thermal unit [g/kWh]
CMEP - Compressor mean equivalent pressure [*bar*]
c_{p,c} - Specific heat at constant pressure of the air
c_{p,s} - Specific heat at constant pressure of burned gas
c_{p,u} - Specific heat at constant pressure of unburned gas
E - Gas expander
EVO - Exhaust valve open
f_{CR} - Correction factor
FMEP - Friction mean effective pressure [*bar*]
G_C - Air mass flow to the supercharged engine [kg/s]
G_E - Electric generator connected to the expander
G_O - Air mass flow to the naturally aspirated engine [kg/s]
ICEV - Internal combustion engine vehicle
IMEP - Indicated mean effective pressure [*bar*]
IMEP_g - Gross indicated mean effective pressure [*bar*]
ISFC - Indicated specific fuel consumption [g/kWh]
IVC - Inlet valve closure
k_s - Isentropic coefficient of the exhaust gas
LHV - Lower heating value of the fuel [MJ/kg]
m₀ - fresh charge mass [kg]
MAP - Manifold absolute pressure [*bar*]
MAP_{max} - Maximum manifold absolute pressure [*bar*]
MGI - Electric motor/generator
MG2 - Electric motor/generator
m_s - residual gas mass [kg]
p_c - boosting pressure [*bar*]
P_{comp} - Power required by the compressor [kW]
P_{exp} - Power produced by the expander [kW]
PMEP - Pumping mean effective pressure [*bar*]
p_s - Engine exhaust pressure [*bar*]
p_{so} - Exhaust pipe pressure [*bar*]
RGF - Residual gas fraction
R_{INT} - Intercooler efficiency
RMEP - Recovery mean equivalent pressure [*bar*]

R_s' - Specific gas constant of exhaust gas or burned gas
 T - Temperature [K]
 T_0 - Air temperature in the intake manifold [K]
 T_1 - In-cylinder gas temperature at IVC [K]
 T_4 - In-cylinder gas temperature at EVO [K]
 T_C - Air temperature at the intercooler outlet [K]
 T'_C - Air temperature at the compressor outlet [K]
 T_R - Residual gas temperature [K]
 T_S - Exhaust gas temperature [K]
 u - normalized mean piston speed
 u_m - mean piston speed [m/s]
 $u_{m,max}$ - maximum mean piston speed [m/s]
 V_A - Engine displacement of the naturally aspirated engine [cc]
 V_{AX} - Engine displacement in the naturally aspirated thermal unit [cc]
 V_{SX} - Engine displacement in the supercharged thermal unit [cc]
 V_T - Engine displacement of the turbocharged engine [cc]
 ϕ - relative MAP = MAP/MAP_{max}
 α - Air-fuel ratio
 α_{ST} - Stoichiometric air-fuel ratio
 β_C - Compressor pressure ration
 β_S - Expander and turbine pressure ratio
 δ_0 - Air density in the intake manifold [kg/m^3]
 δ_C - Density of the compressed air in the intake manifold [kg/m^3]
 ϵ - Number of revolutions per cycle
 η_b - Brake thermal efficiency of the engine
 $\eta_{b,max}$ - Maximum brake thermal efficiency of the engine
 $\eta_{b,TOT}$ - Overall brake thermal efficiency of the thermal unit
 η_C - Compressor efficiency
 η_E - Expander efficiency
 η_{EM} - Electric motor efficiency
 η_i - Indicated thermal efficiency of the engine
 $\eta_{i,max}$ - Maximum indicated thermal efficiency of the engine
 η_m - Overall mechanical efficiency of the engine
 η_T - Turbine efficiency
 λ - Relative air-fuel ratio
 λ_V - Volumetric efficiency of the engine
 $\lambda_{V,C}$ - Volumetric efficiency of supercharged/turbocharged engine
 $\lambda_{V,max}$ - Maximum volumetric efficiency of the engine
 ρ - volumetric compression ratio (naturally asp. engine)
 ρ' - volumetric compression ratio (turbo/supercharged engine)
 ψ - Normalized load variable = $BMEP/BMEP_{max}$

Subscripts

0 - Reference condition
 c - Compression/compressed
 g - Gross
 s - Exhaust gas

Appendix A

Residual Gas Fraction

Considering that at the inlet valve closure, the mass entrapped inside the cylinder is composed by fresh charge (m_0) and exhaust residual gas from previous cycle (m_s), the residual gas fraction RGF represents the ratio between the residual gas mass and the total in cylinder mass:

$$RGF = \frac{m_s}{m_{TOT}} = \frac{m_s}{m_0 + m_s} \quad (67)$$

The fresh charge mass entrapped in the cylinder is correlated to the volumetric efficiency of the engine λ_V hence :

$$m_0 = \lambda_V \cdot \frac{MAP}{R'_0 \cdot T_0} \cdot V \quad (68)$$

where V represents the engine displacement, while MAP and T_0 are the pressure and temperature in the intake manifold. As regards the residual gas mass, the authors assumed that this is represented by the amount of exhaust gas inside the cylinder at the ideal end of the exhaust stroke, i.e. at top dead center. Hence the residual gas mass is evaluated as:

$$m_s = \frac{p_s}{R'_s \cdot T_R} \cdot \left(\frac{V}{\rho - 1} \right) \quad (69)$$

being p_s and T_R the pressure and temperature of the in-cylinder residual exhaust gas, ρ the engine compression ratio and hence $V/(\rho-1)$ the in-cylinder volume at top dead center. For the evaluation of the residual gas temperature T_R , according to the simple approach followed, the authors neglected the heat transfer with in-cylinder wall during the exhaust stroke thus assuming an isentropic transformation:

$$T_R = T_4 \cdot \left(\frac{p_4}{p_s} \right)^{\frac{1-k_s}{k_s}} \quad (70)$$

where T_4 and p_4 are the in-cylinder gas temperature and pressure respectively, when the exhaust valve opens (EVO). As already explained, according to experimental findings also confirmed by data reported in the scientific literature, for a spark ignition engine the ratio T_4/T_1 ranges from 3.5 to 4.5, hence in the calculation performed it was considered the plausible value 4. The isentropic coefficient k_s should be evaluated as function of the exhaust gas composition and temperature, as already described above, starting from [equation \(32\)](#).